PTZ Loading Mechanism based on Nonlinear Adaptive Algorithm

Lang Yun

School of Mechanical Engineering, Hefei University of Technology, Xuancheng 242000, China
2021217006@mail.hfut.cn

Abstract. This paper proposes a new Pan-Tilt-Zoom PTZ UAV loading system, which uses the PTZ to connect with the loading mechanism to protect the cargo in the UAV transportation process. PTZ can eliminate the shaking of the cargo box caused by the movement of the drone, and the cargo box below can provide a relatively independent environment for the transportation of goods, reducing the impact of external weather changes on the transportation of goods. By doing so, it improves the stability of the cargo transportation, thereby increasing the diversity of the cargo transported by the UAV, while reducing the excessive packaging to protect the cargo itself, thereby reducing the cost. This paper mainly uses the three-axis PTZ and loading mechanism based on PID Control Algorithms to design a nonlinear PTZ controller, which can be combined with UAV attitude control system to improve the accuracy of PTZ stability control. In this paper, Solid Works is used for modeling, Ansys for static stress and dynamics analysis, and simulink to verify the feasibility of PID control algorithm. It is proved that the system can effectively ensure the stability of goods in transportation, and provides a new idea for the stable loading of UAVs.

Keywords: Quadrotor UAV, PTZ, Loading Mechanism, PID

1 Introduction

The quadrotor UAV is widely used in air transportation because of its high sensitivity and vertical take-off and landing. With the development of the Internet and e-commerce economy, the logistics industry is facing increasing challenges, high labor costs and inefficient traditional distribution methods and the development of small-batch, personalized product production have put forward higher requirements to the logistics industry [1]. Some retail giants such as Amazon, Meituan, DHL, and some drone logistics companies such as Zipline are gradually starting to pilot or operate drone logistics [2-4]. UAV logistics provides a new freight train of thought for the logistics industry, because UAV logistics has the advantage of ignoring traffic congestion, reducing the time limit of traditional logistics, and can provide a new solution for the "last mile transportation" [5].

A common way to carry goods in UAV transportation is to use a gripper, and the UAV will inevitably shake during transportation because of the environment, its own movement and other factors, if the transport is fragile or sealed incomplete liquid, it is

Y. Wang (ed.), *Proceedings of the 2024 2nd International Conference on Image, Algorithms and Artificial Intelligence (ICIAAI 2024)*, Advances in Computer Science Research 115,
https://doi.org/10.2991/978-94-6463-540-9_42

easy to cause damage or leakage of the goods, bringing uncertainty to the transportation. Ti Chen and Jinjun Shan studied a new four-cable suspended UAV transportation system. Under the action of an adaptive layered controller of the system and the damping effect of cables, compared with single-cable suspended UAV, the system can suppress the vibration of the load to a certain extent [6, 7]. But because the drone is connected to the cargo itself using cables, the system cannot guarantee the safety of the cargo in the event of bad weather. Yong Ren et al. studied the modeling and swing suppression of a helicopter suspension system with a rigid body load. However, the method mentioned in the paper is to control the helicopter's motion trajectory to solve the swing and positioning problems at the same time. Therefore, in order to suppress the load swing, the system energy consumption is large. If applied to UAV loading and transportation, it will greatly reduce the endurance of UAV [8]. In the study on the nonlinear control strategy of UAV when carrying load conducted by M.E. Guerrero-Sanchez et al., they designed two nonlinear controllers and compared them. In their simulation numerical simulation experiment, the nonlinear control strategy reduced the swing peak. And the load swing is attenuated in a short time [6]. The above research has greatly inspired this paper. In order to solve the problems in the above research, this paper proposes a PTZ loading system based on Angle measurement optimized by Kalman filter and PID algorithm control. The system is mainly composed of three-axis PTZ and cargo loading box. The algorithm of the head is used to reduce the swing of the load without controlling the attitude of the four-rotor UAV, thus increasing the endurance of the UAV. The cargo box of the load also provides a good environment for it, so that the cargo is free from the impact of bad weather. At the same time, the cargo box can be flexibly replaced when transporting different goods, further improving the applicability of the loading system.

2 Structural Design

2.1 Overall Structure Scheme

The loading mechanism is mainly composed of a shock absorber component, a yaw axis component, a roll axis component, a pitch axis component and a loading component. Figure 1 shows the final assembly model diagram of the whole loading mechanism. The damping component connects the UAV with the whole mechanism through bolts; The damping assembly, the heading shaft assembly, the heading shaft assembly, the transverse roller assembly, the horizontal roller assembly and the pitching shaft assembly are connected by direct drive motor; The pitch shaft assembly comprises a pitch head arm and a slider that can slide on the pitch head arm. The loading assembly is connected to the whole PTZ by bolts. The pitch shaft assembly has structural hard limit and realizes single-arm sliding adjustment of the pitch shaft by sliding block to realize the center of gravity adjustment in the Y direction. Between the slider and the connecting arm, between the connecting arm and the load box are filled with vibration damping columns to reduce the small high-frequency vibration during transportation [9].

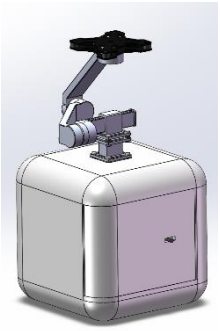

Fig. 1. Final assembly model diagram

2.2 Vibration Reduction Component Design

The damping component is composed of an upper damping plate, damping columns and a lower damping plate, and each part is connected with a screw. The upper vibration damping plate is shown in Figure. 2(a), and the material of the upper vibration damping plate is carbon fiber. The vibration damping column is shown in Figure. 2(b) and is made of rubber. The lower vibration damping plate is shown in Figure. 2(c), which is also made of carbon fiber. The assembly diagram of the shock absorber is shown in Figure. 2(d) The shock absorber can reduce the influence of high-frequency vibration of the UAV on the stability of the head.

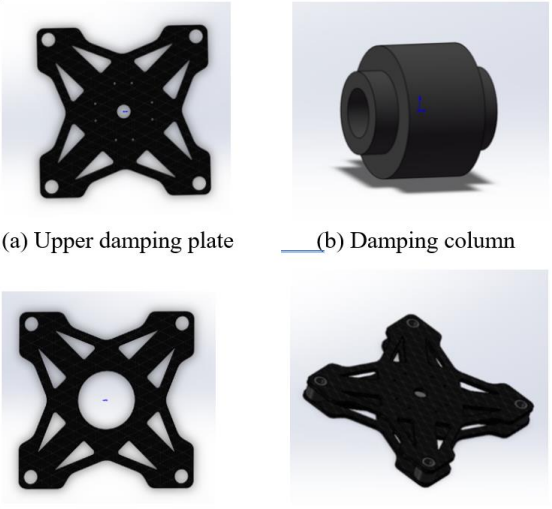

Fig. 2. Vibration reduction component design: (a) Upper damping plate; (b) Damping column; (c) Lower damping plate; (d) The assembly diagram of the shock absorber

2.3 Heading Shaft Assembly Design

As shown in Figure 3, the heading shaft component is mainly composed of a rolling motor and a heading arm. The heading arm is hollowed-out to achieve weight reduction. In order to ensure sufficient stiffness and small mass of the heading arm, the heading arm is made of aluminum alloy; The end of the heading arm is firmly connected with the stator of the rolling motor, and a fixed base plate consisting of two cylindrical protrudes and a slot in the center is installed on the rotor of the rolling motor for connection with the horizontal roller assembly and the base plate is connected with the motor by screws. The component is mainly used to control the direction of the heading axis of the transport object.

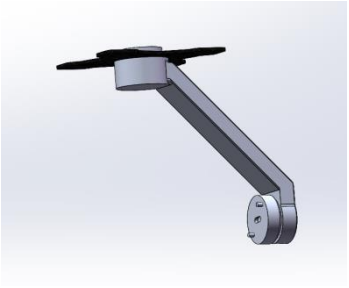

Fig. 3 Heading shaft assembly

2.4 Horizontal Roller Assembly Design

As shown in Figure 4, the horizontal roller component is mainly composed of a pitching motor and a roll arm. The interior of the roll arm is hollow-holed to achieve weight reduction. In order to ensure that the roll arm has sufficient stiffness and small mass, the roll arm is made of aluminum alloy. The top of the rolling arm is provided with two cylindrical grooves matched with the bottom plate of the rolling motor and an ordinary round head flat key protruding; The end of the roll arm is fixed to the pitch motor stator, and a fixed base plate comprising two cylindrical protrudes and a slot in the center is installed on the pitch motor rotor for connection with the pitch shaft assembly, and the base plate is connected to the motor by screws. The structure of the roll assembly ensures that the direction of the cargo box on the roll axis is controlled by the transverse roller motor.

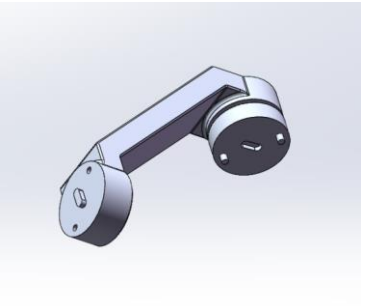

Fig. 4. Horizontal Roller Assembly

2.5 Pitch Shaft Assembly Design

As shown in Figure 5, the pitching shaft assembly is mainly composed of the pitching arm and the sliding block of the pitching arm. The pitching arm is hollow-out to achieve the purpose of weight reduction. In order to ensure that the pitching arm has sufficient stiffness and small mass, the pitching arm is made of aluminum alloy. The top of the pitching arm is provided with two cylindrical grooves matched with the bottom plate of the pitching motor and a common round head flat key protruding. There are two sliding slots for installing the slider in each plane of the pitching arm. There is a hard limiting device at the end of the pitching arm to prevent the slider from exceeding the predetermined position. The whole pitch shaft assembly is used to connect the PTZ and the load mechanism below, and through the combination of its top and the pitch motor, the movement of the load in the direction of the pitch axis is controlled.

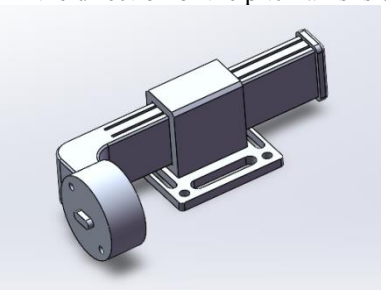

Fig. 5. Pitch shaft assembly

2.6 Loading Assembly Design

The loading assembly as shown in Figure 6(a) is mainly composed of a loading box, a connecting arm and a vibration damping column. The connecting arm is connected with the upper slide block and the lower loading box by bolts. In order to fix the loaded goods, Velcro stickers are installed at the bottom of the loading box, as shown in Figure 6(b) and Velcro straps can be installed on the goods to fix them inside the loading box. In order to reduce the quality of the entire structure as much as possible, the loading box is made of nylon, the connecting arm is hollow design and aluminum alloy material,

and the vibration damping column is made of rubber.

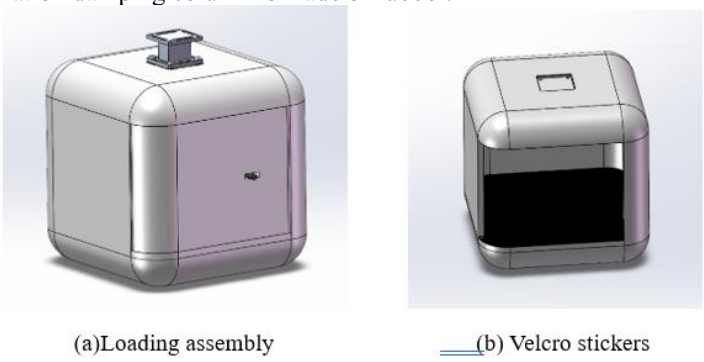

Fig. 6. Loading assembly design: (a)Loading assembly; (b) Velcro stickers

3 Static Simulation Analysis

The structure of the head is all 6061 aluminum alloy, and the allowable stress of 6061 aluminum alloy is 165MPa. The model was analyzed statically by using ANSYS Workbench. In order to reduce the amount of finite element calculation, mass points are added on the end face of the pitch shaft joint direct drive motor according to the actual mass and center of mass position of each component [9].

3.1 Static Analysis of Heading Shaft Assembly

Figure 7 (a) is the loading diagram of the model. The top of the heading axis is fixed, and a force of 50N in the vertical direction is applied to its end. Finally, the effective strain and effective stress diagrams can be obtained as shown in Figure 7 (b) and (c) respectively. Through the analysis of the image calculation, it can be seen that the maximum elastic strain of the heading axis is 9.3x10^ (-5) mm, and the maximum stress is 6.4421MPa. The deformation and stress both meet the allowable material requirements and the functional requirements of the head.

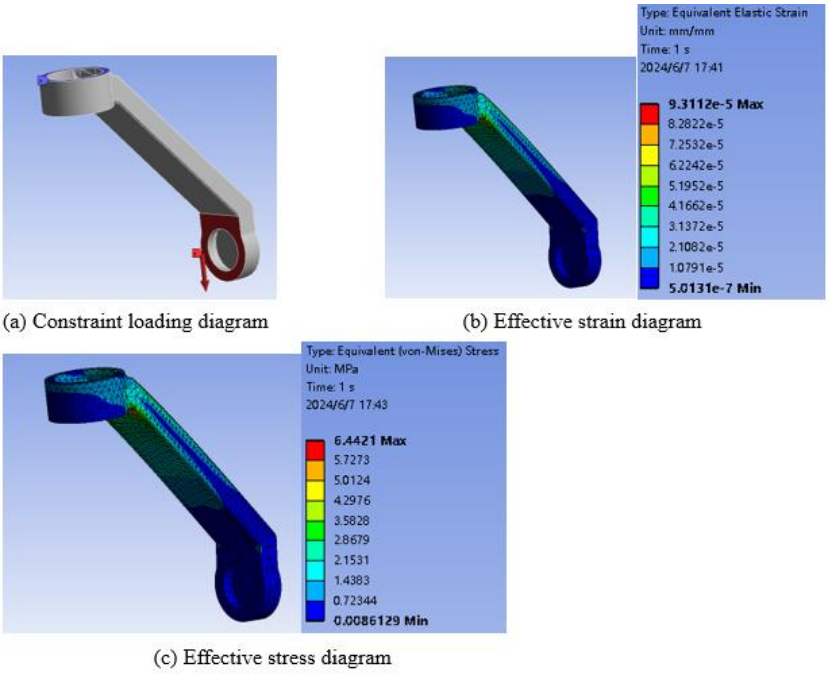

(a) Constraint loading diagram (b) Effective strain diagram

(c) Effective stress diagram

Fig. 7 Static analysis of heading shaft assembly: (a) Constraint loading diagram; (b) Effective strain diagram; (c) Effective stress diagram

3.2 Static Analysis of Horizontal Roller Assembly

As shown in Figure 8(a), the model loading diagram is fixed at the connection between the horizontal roller and the motor, and 50N vertical downward force is applied to its end. Eventually, the effective strain and effective stress diagram can be obtained as shown in Figure 8(b) and (c) respectively. Through the analysis of the image calculation, it can be seen that the maximum elastic strain of the heading axis is 1.1x10^(-4) mm, and the maximum stress is 7.8293MPa. The deformation and stress both meet the allowable material requirements and the functional requirements of the head.

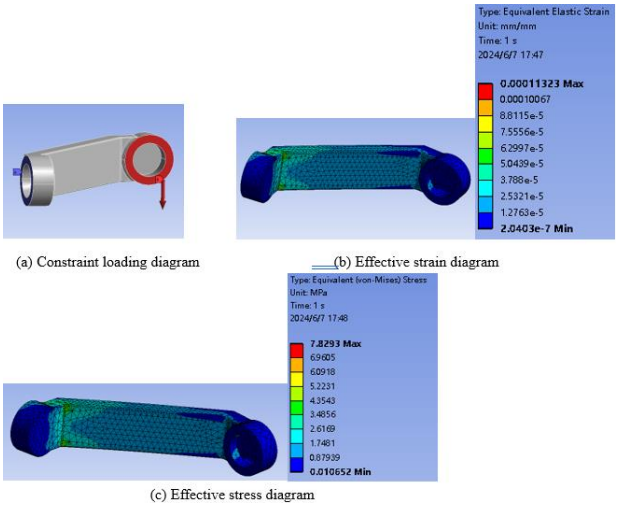

Fig. 8. Static analysis of horizontal roller assembly: (a) Constraint loading diagram; (b) Effective strain diagram; (c) Effective stress diagram

3.3 Static Analysis of Pitch Shaft Assembly

As shown in Figure 9(a), the model loading diagram is fixed at the connection point between the pitch shaft and the motor, and a vertical downward force of 12.5N is applied to the four connection holes on the end face of the lower slide block respectively. Finally, the effective strain and effective stress diagram can be obtained as shown in Figure 9(b) and (c) respectively. Through the analysis of the image calculation, it can be seen that the maximum elastic strain of the heading axis is 2.4x10^ (-4) mm, and the maximum stress is 4.4526MPa. The deformation and stress both meet the allowable material requirements and the functional requirements of the head.

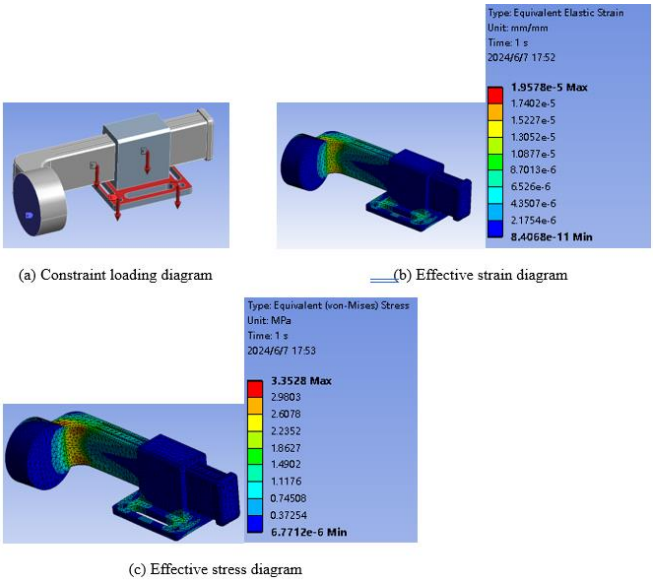

(a) Constraint loading diagram (b) Effective strain diagram

(c) Effective stress diagram

Fig. 9. Static Analysis of pitch shaft assembly: (a) Constraint loading diagram; (b) Effective strain diagram; (c) Effective stress diagram

4 Dynamic Simulation Analysis

In order to reduce the amount of finite element calculation, a total of 33,677 nodes and 16,240 units were divided in this analysis. The analysis structure of PTZ model is shown in Figure 10(a). By using ANSYS Workbench to simulate the mounting of 100N heavy objects under PTZ, rotary connection pairs were applied to the transverse roller motor and the pitching shaft motor. Let both the transverse roller and the pitch shaft rotate 30 degrees within 1S, and the specific constraint diagram is shown in Figure 10(b), from which the following analysis can be obtained.

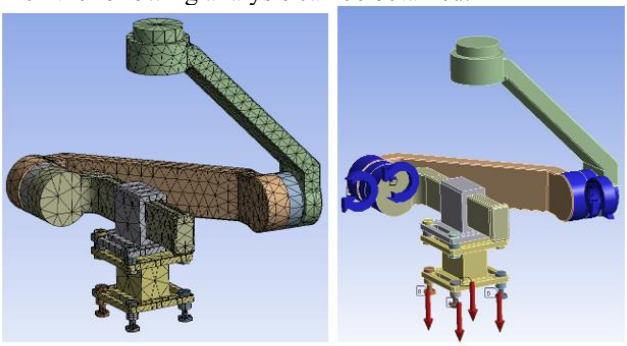

(a) Unit division diagram (b)constraint diagram

Fig. 10. Analysis diagram: (a) Unit division diagram; (b)constraint diagram

4.1 Total Deformation

As shown in Figure 11, the figure shows the total deformation of PTZ after movement, which also includes the displacement changes of each part relative to the initial state. It can be seen that the linearity of the movement of each axis is good, and the attitude control of the transport box has been completed.

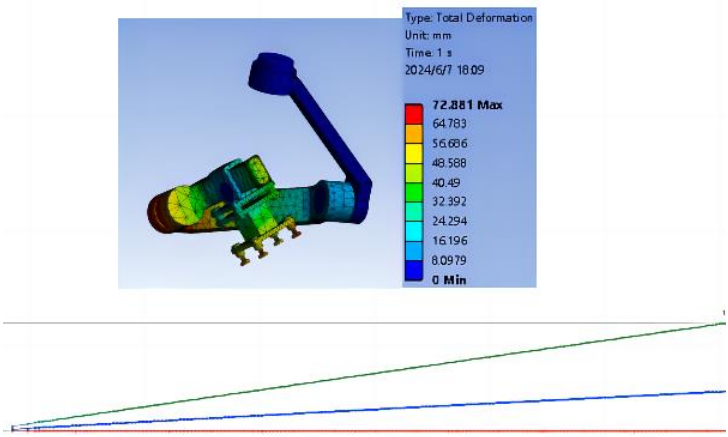

Fig. 11. Total deformation

4.2 Equivalent Elastic Strain

As shown in Figure 12, the maximum elastic equivalent strain is about 1.01x10-3mm, which can meet the application requirements. The equivalent strain oscillates slightly in the initial phase of movement, but quickly returns to linear changes, indicating that the system is controllable enough to meet the control requirements of the payload tank.

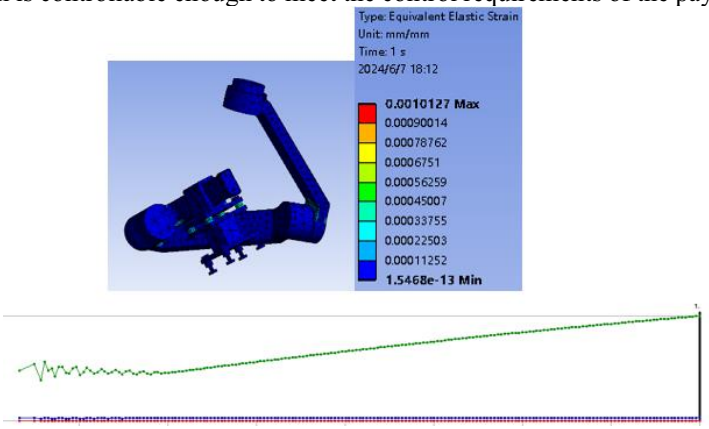

Fig. 12. Equivalent elastic strain

4.3 Equivalent Stress

Similar to the elastic equivalent strain, as shown in Figure 13, the elastic stress also experienced an initial shock, but quickly returned to a linear change, indicating that the system was stable enough to complete the control of the compartment.

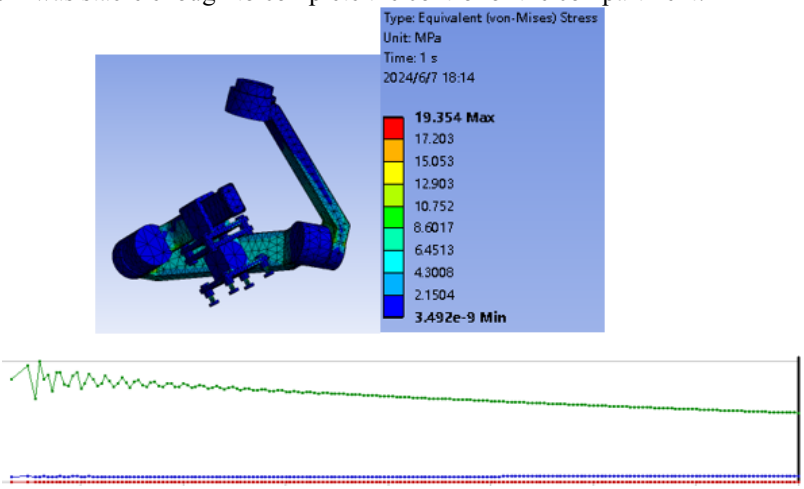

Fig. 13. Equivalent stress

5 PTZ Control System

In this paper, the system is designed and verified by means of simulation, as shown in Figure 14, which is a function modeling of the attitude control of the payload box, some parameters of which can be modified according to the actual situation [10]. Figure 15 shows the nonlinear adaptive control algorithm model built according to Lyapunov's method. A function is input to it, and the final simulation result is shown in Figure 16. As can be seen from Figure. 16, the algorithm can effectively track input and realize real-time control of PTZ.

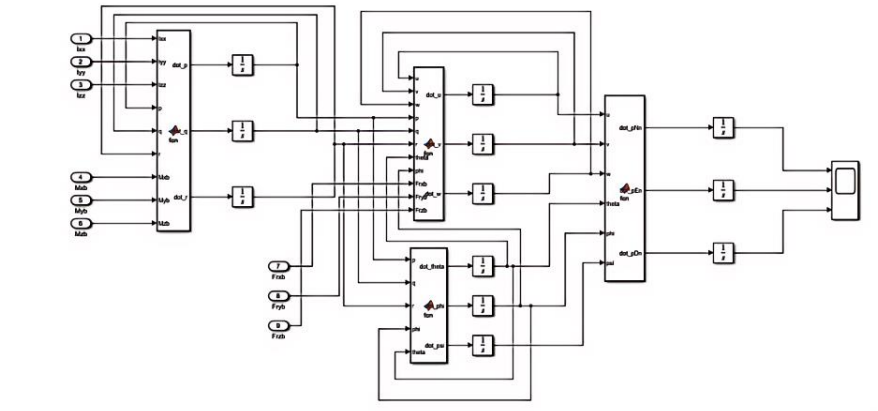

Fig. 14. Payload box attitude control model

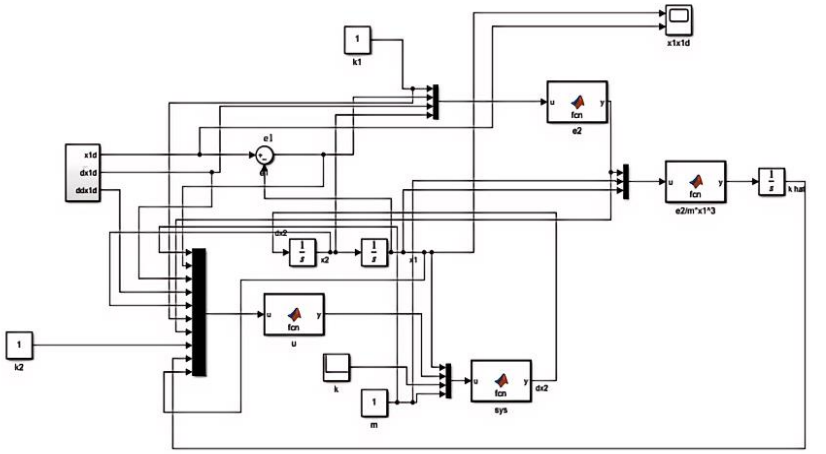

Fig. 15. Nonlinear adaptive control algorithm model

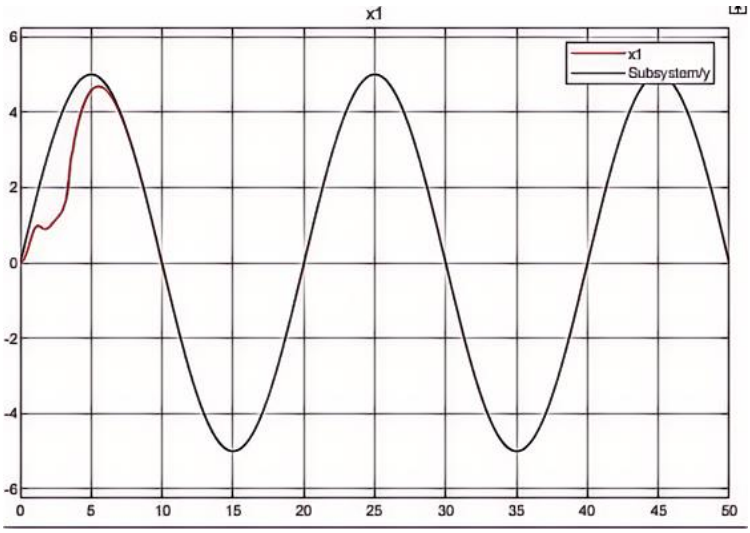

Fig. 16. Algorithm simulation result

6 Conclusion

In this paper, Solid Works is used for modeling, Ansys for static stress and dynamics analysis, and simulink to verify the feasibility of PID control algorithm. It is proved that the system can effectively ensure the stability of goods in transportation, and provides a new idea for the stable loading of UAVs.

For the four-rotor UAV in the transport operation, the cargo will be affected by the UAV movement and external environmental factors. Inspired by the design of the head of the camera UAV, the impact of the movement of the UAV is reduced by the head of the PTZ, and the impact of the external environment is reduced by the cargo box. Through the static and dynamic analysis of the PTZ, the feasibility of the PTZ in freight transportation is verified, and the good stability of the PTZ is verified by the simulation of PID algorithm. It provides reference for the development and iteration upgrade of stable PTZ of the same type.

References

1. He Liming: Strategic Considerations of effectively reducing the logistics cost of the whole society. China's Circulation Economy
2. Zipline Drone Delivery & Logistics (flyzipline.com)
3. Amazon releases updates on drone delivery, robots, and packaging (aboutamazon.com)
4. https://www.meituan.com/technology
5. Borghetti F, Caballini C, Carboni A, Grossato G, Maja R, Barabino B. The Use of Drones for Last-Mile Delivery: A Numerical Case Study in Milan, Italy. Sustainability. 14(3), 1766 (2022).

6. Guerrero-Sánchez, M. E. Lozano, R. Castillo, P. et al. Nonlinear control strategies for a UAV carrying a load with swing attenuation. Applied Mathematical Modelling 91, 709-722 (2021).
7. Recalde LF, Guevara BS, Carvajal CP, Andaluz VH, Varela-Aldás J, Gandolfo DC. System Identification and Nonlinear Model Predictive Control with Collision Avoidance Applied in Hexacopters UAVs. Sensors (Basel). 2022;22(13):4712.
8. Ren Y, Li K, Ye H. Modeling and anti-swing control for a helicopter slung-load system. Applied Mathematics and Computation 372, 124990 (2020).
9. Hui Y, Yu H, Ye J. Design and Research of Light, Small and High Precision Airborne Stable Head[J]. Machine Design & Manufacturing Engineering 53(02), 28-33 (2024).
10. Yang C, Liang J. Multi-rotor UAV Design, 113-130 (2018).